International Journal of Automotive Technology, Vol. 6, No. 2, pp. 133–139 (2005)

1229-9138/2005/020-07

SIMULATION OF KNOCK WITH DIFFERENT PISTON SHAPES IN A HEAVY-DUTY LPG ENGINE

H. CHOI[1], J. LIM[1], K. MIN[1]* and D. LEE[2]

[1]School of Mechanical and Aerospace Engineering, Seoul National University, Seoul 151-742, Korea
[2]Department of Mechanical Engineering, Inha University, Incheon 402-751, Korea

(Received 8 October 2003; Revised 30 October 2004)

ABSTRACT–In this study, a three-dimensional transient simulation with a knock model was performed to predict knock occurrence and autoignition site in a heavy-duty LPG engine. A FAE (Flame Area Evolutoin) premixed combustion model was applied to simulate flame propagation. The coefficient of the reduced kinetic model was adjusted to LPG fuel and used to simulate autoignition in the unburned gas region. Engine experiments using a single-cylinder research engine were performed to calibrate the reduced kinetic model and to verify the results of the modeling. A pressure transducer and a head-gasket type ion-probe circuit board were installed in order to detect knock occurrences, flame arrival angles, and autoignition sites. Knock occurrence and position were compared for different piston bowl shapes. The simulation concurred with engine experimental data regarding the cylinder pressure, flame arrival angle, knock occurrence, and autoignition site. Furthermore, it provided much information about in-cylinder phenomena and solutions that might help reducing the knocking tendency. The knock simulation model presented in this paper can be used for a development tool of engine design.

KEY WORDS : 3-dimensional simulation, Knock, Auto-ignition, Reduced kinetic model, Combustion model

1. INTRODUCTION

It is likely that air pollution would worsen in the urban area as the number of diesel vehicles increases. Consequently, reducing the exhaust emissions of heavy duty diesel vehicles has become a very important issue. LPG has been well known as a clean alternative fuel for vehicles (Dardalls *et al.*, 1998). Recently, several LPG engines for heavy-duty vehicles, which can replace some diesel engines which are the main sources of air pollution in urban areas, has been developed. In order to develop an advanced heavy-duty LPG engine, the liquid phase LPG injection (LPLI) system which can achieve higher power, higher efficiency, and lower emission characteristics than an existing mixer system, was adapted as a fuel supply system for a heavy-duty engine (Kang *et al.*, 2001). Then, the combustion characteristics regarding the injection of a LPG fuel as well as flow characteristics for intake port and various piston cavities were investigated and optimized to enhance engine performance and at the same time lower the exhaust emissions (Kim *et al.*, 2002; Kang *et al.*, 2001).

However, although LPG fuel has a high octane number, the increase in compression ratio and advance of sparking timing, which can improve engine performance, are limited by engine knock. That is because the cylinder bore size of heavy-duty LPG engines is larger than that of conventional SI engines (Kang *et al.*, 2001; Hwan *et al.*, 2001). It is well known that engine knock originates from the autoignition of the end gas which causes extremely rapid energy release, resulting in a localized high pressure region. The non-uniformity of this pressure distribution causes the pressure wave to propagate from the end gas region across the combustion chamber. This causes physical damage to the piston and combustion chamber, and lowers the thermal efficiency (Lee *et al.*, 2000; Chun and Kim, 1994). Hence, the study of knock characteristics has become essential for the development of a heavy-duty LPG engine.

Many researches about engine knock pheonmena have been done in our laboratory. The knock characteristics of a heavy-duty LPG engine were investigated with various engine speeds, air excess ratios and LPG fuel compositions (Hwan *et al.*, 2001). Moreover, the knock position was estimated with a head gasket type ion-probe in the same engine (Lee *et al.*, 2002).

However, it is necessary to develop a tool which can predict engine knock and autoignition sites during the design stage of engine, to cut engine development cost. It has become possible to simulate flame propagation,

*Corresponding author. e-mail: kdmin@snu.ac.kr

Table 1. Engine specifications.

Engine type	LPLI single cylinder engine
Combustion system	Spark Ignition
Combustion chamber	Bowl-in-piston
Bore × Stroke	130 × 140 mm
Displacement volume	1.85 liter/cyl.
Compression ratio	10.0
IVO, IVC	18° BTDC, 50° ABDC
EVO, EVC	50° BBDC, 18° ATDC

which approximates real phenomena more closely and develop a knock model which can predict knock occurrence and autoignition site in spark ignition engines, with the recent development of a turbulent combustion model and a low-temperature chemistry mechanism (Lee *et al.*, 2000).

The objective of this paper was to develop a tool that predicts knock occurrence and autoignition sites in heavy-duty LPG engines, and to optimize piston shape. A turbulent premixed combustion model was used to simulate flame propagation in the combustion chamber. A reduced kinetic model for autoignition was implemented to simulate the low temperature chemistry in the unburned gas region.

2. THREE-DIMENSIONAL SIMULATION

This study was carried out using a naturally aspirated spark ignition LPG engine, which was originally designed as a compression ignition engine. The specifications of the engine are listed in Table 1.

The computational moving mesh which consisted of approximately 303,000 cells at BDC including the intake and exhaust ports, was constructed with valve and piston motions as shown in Figure 1. In order to maintain good mesh quality during the calculation, the event technique was used to make cell layer in the cylinder liner and valve moving regions be removed or added with the piston and valve motions (Adapco software Limited, 1999).

A multipurpose flow simulation package STAR-CD was used, and combustion and autoignition models were added as subroutines. The standard k-ε model was used as the turbulence model with the algebraic "law of wall" representation of flow, heat and mass transfer within the boundary layers.

All calculations were performed at the engine speed of 1,200 rpm, stoichiometric, and at full load condition (WOT). The spark timing was determined as 12° BTDC where knock occurs during engine experiments with base pistons (Hwan *et al.*, 2001). The calculation started with the opening of the intake valve. The boundary conditions of the intake and exhaust pressures were obtained from a one-dimensional thermodynamic calculation using BOOST (AVL, 2000).

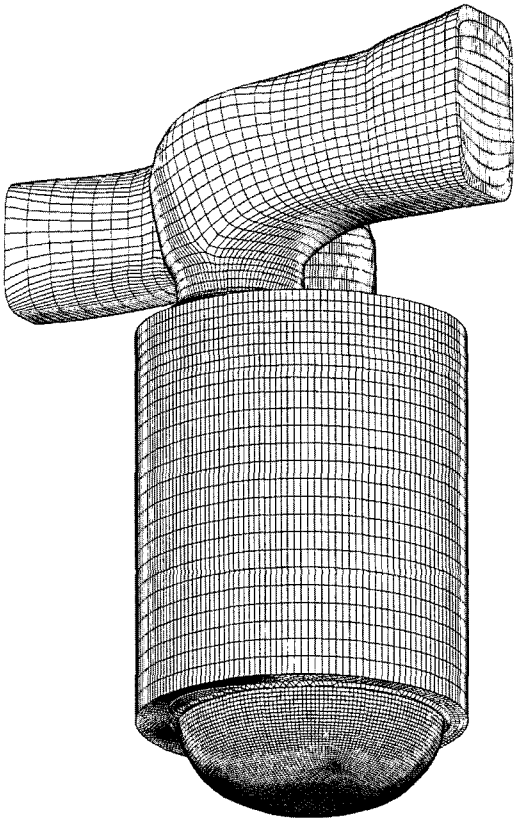

Figure 1. Computational mesh of heavyduty LPG engine.

2.1. Piston Shape

To optimize the combustion cavity, three piston cavities were tested: Base (dog-dish) type, bathtub type, and modified type pistons with a compression ratio of 10.0. Figure 2 shows the shapes of these pistons and some of their specifications. The bathtub piston had the largest squish area, which was expected to produce the highest level of turbulence at the end of the compression stroke. The modified piston had a shape compromising base whereas the bathtub pistons had the smallest squish area.

2.2. Combustion Model

Weller introduced an FAE model for premixed turbulent combustion, which simulates the growth of the initial flame kernel into a fully developed turbulent flame and its subsequent propagation (Weller *et al.*, 1994) (Heel *et al.*, 1998). The model assumes that the reaction zone is thin and laminar, and that the increased reaction area is responsible for the burning rate. The transport equation for the progress variable c, which is equal to 0 in the fully unburned gas and 1 in the fully burned gas, can be expressed as follows:

squish area: 3,259 mm^2
piston surface area: 17,178 mm^2
top land: 15.68 mm

(a) Base piston

squish area: 4,637 mm^2
piston surface area: 20,397 mm^2
top land: 15.68 mm

(b) Bathtub piston

squish area: 2,601 mm^2
piston surface area: 18,356 mm^2
top land: 15.68 mm

(c) Modified piston

Figure 2. Variation of piston shapes in 3-dimentsional computation.

$$\frac{\partial(\bar{\rho}\tilde{c})}{\partial t}+\nabla\cdot(\bar{\rho}\tilde{\vec{u}}\tilde{c})-(\bar{\rho}\tilde{D}_c\nabla\tilde{c})=S_c+S_I+S_Q+S_k \quad (1)$$

The RHS of Equation (1) represents the source terms of progress variable. S_I is the ignition source term and S_Q is the flame quenching source near wall (Lee *et al.*, 2000; Poinsot *et al.*, 1993). The local fuel consumption rate $S_{\bar{c}}$ in Equation (1) can be related to the flame wrinkle factor Ξ by

$$S_{\bar{c}}=\rho_u\Xi S_l|\nabla\tilde{c}| \quad (2)$$

where ρ_u is the unburned gas density and Ξ is obtained from Herweg's semi-empirical correlation (Herweg *et al.*, 1992), which can be expressed as:

$$\Xi=1+A\left(\frac{u'}{u'+S_l}\right)^{1/2}\left(1-\exp\left(-\frac{t}{\tau}\right)\right)^{1/2}\times\left(1-\exp\left(-\frac{S_l}{u'+S_l}\frac{t}{\tau}\right)\right)^{1/2}\left(\frac{u'}{S_l}\right)^{5/6} \quad (3)$$

Here t is the time after the ignition, τ is a characteristic time scale, and A is the empirical constant. In addition, turbulence intensity u' is obtained from the turbulent kinetic energy with the assumption that the turbulence is isotropic. The laminar burning velocity S_l is obtained from Pae and Min's correlation (Pae and Min, 2001). The other details about Equation (1)~(3) and wall-quenching mechanism were presented in the prior studies (Weller *et al.*, 1994; Kamarados, 1994; Poinsot *et al.*, 1993).

2.3. Autoignition Model

A reduced kinetic model for autoignition was implemented to calculate the unburned gas temperature rise in the low temperature range, from 700 K to 1,200 K (Cowart *et al.*, 1990). As summarized in Table 2, this mechanism consists of 17 chemical species and 19 chemical reactions. The essential features of this model are that it can reproduce two stages hydrocarbon ignition characteristics under high pressure. Moreover, it includes the effect of various fuel structures by adjusting the forward activation energy of the isomerization reaction (reaction 3 in Table 2) (Lee *et al.*, 2000). We calibrated E_3^+ to match the predicted knock onset angle with measured data.

Table 2. Reduced kinetic model for autoignition (Cowart *et al.*, 1990).

	Reactions	$-\Delta H_f$ (kcal/mol)	Log A^+ (cm^3/mol s)	E_a^+ (kcal/mol)	Log A^- (cm^3/mol s)	E_a^- (kcal/mol)
1	RH + $O_2\leftrightarrow$ R· + HO_2·	46.4	13.5	46	12	0
2	R· + $O_2\leftrightarrow RO_2$·	−31	12	0	13.4	27.4
3	RO_2·↔R·OOH (fuel)	7.5	11	20.8	11	11
4	R·OOH + $O_2\leftrightarrow O_2$ROOH·	−31	11.5	0	13.4	27.4
5	O_2ROOH·→OROOH + OH·	−26.6	11.3	17	-	-
6	RH+OH·→R· + H_2O	−23.5	13.3	3	-	-
7	OROOH→ORO· + OH·	43	15.6	43	-	-
8	R· + $O_2\leftrightarrow$Olefin + HO_2·	−13.5	11.5	6	11.5	19.5
9	HO_2· + HO_2·→H_2O_2· + O_2	−38.5	12.3	0	-	-
10	H_2O_2· + M→OH + OH + M	51.4	17.1	46	-	-
11	ORO·→R'CHO· + R·'	8.5	14	15	-	-
12	RO_2·+ HO_2·→ROOH + O_2	−38.5	12	0	-	-
13	R·OOH→OH + R'CHO· + Olefin	−3	14.4	31	-	-
14	RO_2· + R'CHO·→ROOH + R'CO	−0.6	11.45	8.6	-	-
15	RH + RO_2·↔R· + ROOH	8	11.2	16	10.1	8
16	HO_2· + R'CHO·→H_2O_2· + R'CO	−0.6	11.7	8.6	-	-
17	RH + HO_2·↔R· + H_2O_2·	8	11.7	16	10.8	8
18	HO_2· + Olefin→EPOX + OH	−0.23	10.95	10	-	-
19	R· + R·→RH	−85	13.2	0	-	-

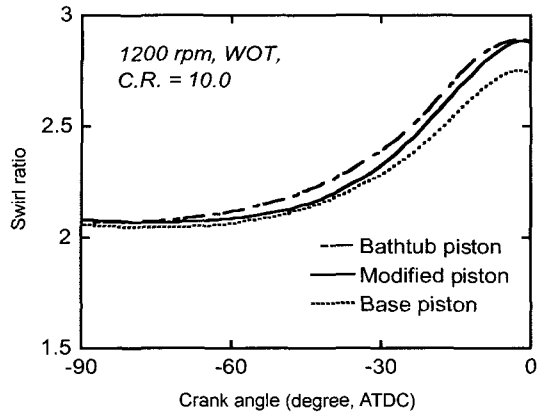

Figure 3. Swirl ratios in various combustion chamber shapes at 1,200 rpm and WOT.

During simulation, autoignition occurred where the temperature of cells reaches 1,200 K before the arrival of the flame (Chun *et al.*, 1988). After autoignition, a specific mass burning rate of the fuel, S_k was given into the calculation cell in Equation (1). Engine knock was determined when the cylinder pressure rising rate was greater than 0.5 MPa/CA deg with the autoignition source term (Lee *et al.*, 2000). Consequently, this model could predict the knock occurrence and the location of the autoignition site.

3. SIMULATION RESULTS

3.1. Flow Field

In this work, the heavy-duty LPG engine had a helical intake port which produced a high level of swirl flow during the intake stroke. The shapes of the intake port and valve control the swirl ratio dominantly, prior to the flow entering the cylinder (Heywood, 1988). There was no significant difference among swirl ratios during the intake stroke. At the compression stroke, the volume fraction of the piston bowl in the combustion chamber increased, and the piston bowl shape influenced swirl flow gradually. As shown in Figure 3, the difference of swirl ratio between the base and bathtub pistons was 4.8%. the swirl ratio of modified piston existed between the values of base and bathtub pistons. Figure 4 shows by section, the flow field at TDC in the combustion chamber. In the view from the engine top, the direction of swirl flow was clockwise, and its center was located near the spark plug in all cases.

As the piston moved up, increasing swirl ratio grew due to conserve angular momentum (Heywood, 1988). Moreover, the interaction between the swirl and the squeezed flow from the squish at the end of compression stroke produced additional turbulence. The bathtub

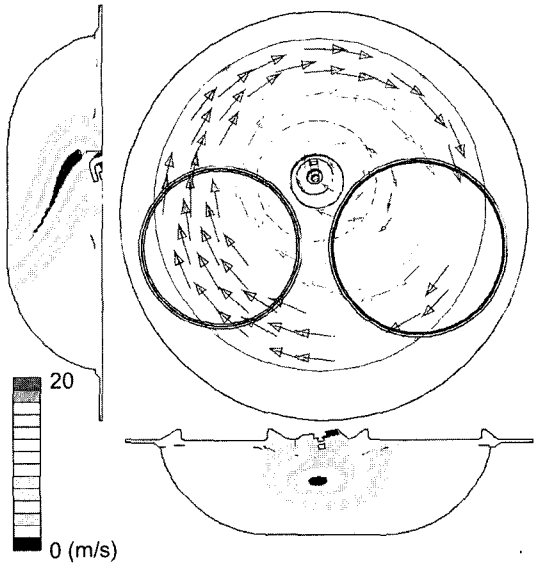

Figure 4. Sectional distribution of flow field in the base piston, at 1,200 rpm and WOT.

piston had the highest swirl ratio and largest squish area, accordingly the turbulent intensity was the highest. The turbulent energy of base piston was 4.1 m^2/s^2 at TDC, and that of the bathtub piston was 10.6% larger than that of base piston. The modified piston had a 3.4% smaller turbulent kinetic energy than the base piston because of its smallest squish area.

3.2. Flame Propagation

Figure 5 shows the flame propagation in cross section of piston bowl top. The location of spark plug was offset from the cylinder center toward the intake port side by 11 mm, avoiding the interference of valves. Thus, the distance between the spark plug and the cylinder wall of the exhaust port side was longer than that of the intake port side. Simulation results showed that the flow field enhanced slightly the flame propagation toward the intake port side. Therefore, the flame reached the intake port side of the piston bowl wall for the first time and propagated into the squish, while a large amount of fuel-air mixture remained unburned in the exhaust port side. Autoignition due to compression occurred at unburned mixture within squish before the arrival of the flame. Although the flame arrival time to the intake port side was shorter than to the exhaust port side, unburned mixture remained in all squish of the combustion chamber at the time the knock occurred. That was due to the very large bore size of LPG engine. Autoignition could have occurred anywhere in the squish rigion.

Figure 6 shows the flame propagations with the engine crank angle of the base, bathtub, and modified type piston cavities. Compared with the base piston, flame propa-

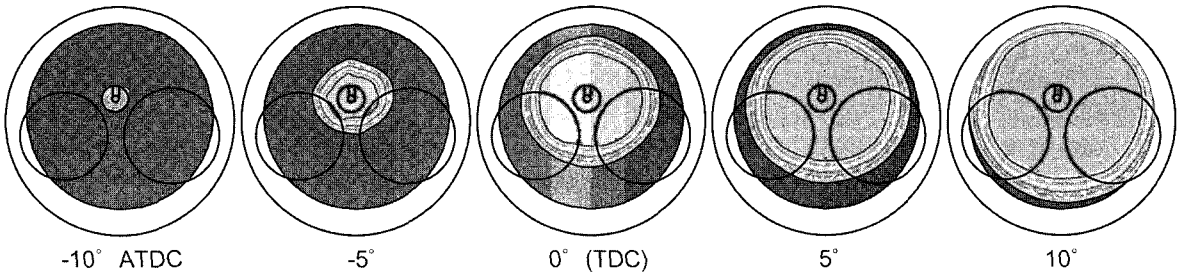

Figure 5. Sectional contour of progress variable in the base piston bowl at 1,200 rpm, WOT, compression ratio of 10.0, and spark timing of 12° BTDC.

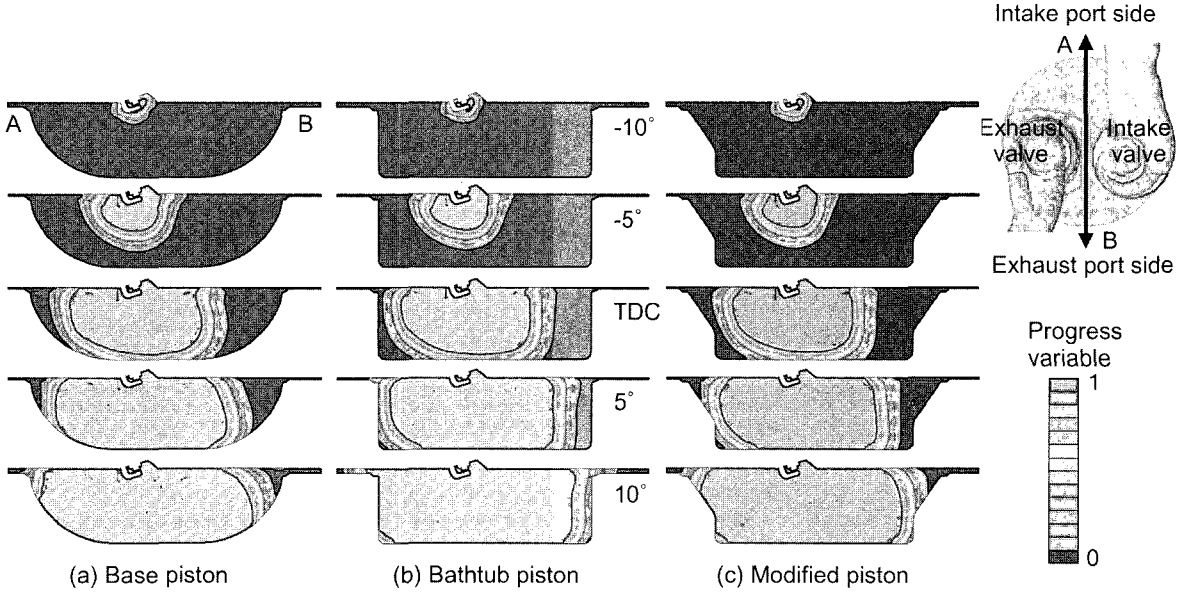

Figure 6. The side view of flame propagation process with a variation of piston cavities at 1,200 rpm, WOT, compression ratio of 10.0, and spark timing of 12° BTDC.

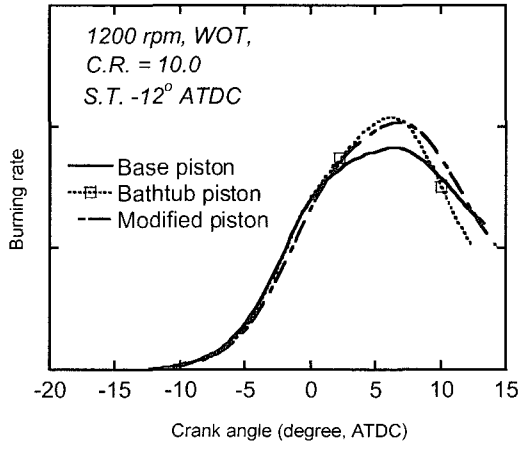

Figure 7. The comparison of reaction rates with base, bathtub, and modified pistons at compression ratio of 10.0, 1,200 rpm, WOT, and spark timing of 12° BTDC.

gation in the bathtub piston showed larger surface area after TDC, when flame reached the bottom of the piston bowl. After that, the flame propagating surface was restricted in the base piston by shallowing bowl depth. On the other side, the bathtub shape maintained flame front surface almost constant until the flame arrived at the side wall of the piston bowl. Figure 7 shows the comparison of the relative burning rates along the crank angle. From TDC to 10° ATDC, the burning rate in the base piston was lower than that in the bathtub piston. In the modified piston, the burning rate had a combined feature from both base and bathtub pistons, by the way its flame propagation developed slightly later than in other pistons due to its smallest turbulence.

3.3. Autoignition Occurrence

In the bathtub piston, autoignition occurred at 10.8° ATDC. This prediction of autoignition onset time was

Table 3. Autoignition onset angle in calculation.

Piston type	Base	Bathtub	Modified
Autoignition onset angle (ATDC)	12.0°	10.8°	13.6°
Mass fraction burned	84.5%	82.0%	88.9%

faster than that in base bowl by 1.2° due to the rapid burning process. Table 3 shows the crank angle when autoignition occurred first, and the mass fraction burned in each piston. In the modified piston, the autoignition onset time was later than in the base piston by 1.6°. In this work, autoignitions occurred in all pistons. However, autoignition did not necessarily cause knock in all cases. In the base and bathtub pistons, the unburned gas fractions were 15.5% and 18.0% respectively when autoignition occurred. These autoignitions were able to develop into knocks. While, the autoignition in the modified piston could not convert to knock, because it occurred at the end of combustion (13.6° ATDC) when 88.9% of fuel mass had burned, and the unburned gas fraction seemed to be too small to increase the cylinder pressure sharply (Lee *et al.*, 2000). Therefore, adopting the modified piston could possibly reduce knock occurrence by its smaller turbulence characteristic.

3.4. Autoignition Site

Figure 8 shows flame and autoignitions in base piston at 12° ATDC. Autoignitions occurred at several locations in the squish region. It also took place in the squish of the intake port side. However, the autoignition of the intake port side failed to develop into a knock. I nstead, the autoignition accerated the flame propagation because it was too close to the flame surface. At the other side, autoignition occurred ahead of the flame front in the other squish region, and developed independently into knock. In other pistons, like in the base piston, autoignitions occurred at several sites in the squish area, especially in exhaust port side.

The simulation results of the flame propagation and autoignition position were compared with the engine experimental data (Choi *et al.*, 2002). Averaged flame contours and knocking probabilities are shown in Figure 9. Flame contour indicates in the figure that propagating speed was fastest in the direction of 1 o'clock in the figure. Knock probability was measured at 6 locations around the cylinder wall by using ion-probes (Choi *et al.*, 2002). Knocks were detected in all measurement points, however knock probabilities in the intake port side (position 1 and 2) were relatively low, while they were higher values in the other positions (3~6 in Figure 9) where the flame arrived later and the squish area was larger than the intake port side. The simulation concurred well with these phenomena.

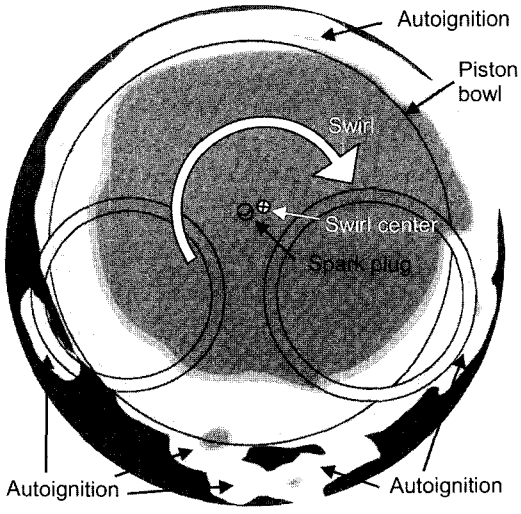

Figure 8. The locations of autoignition onset at 12° ATDC at 1,200 rpm, WOT, and spark timing of 12° BTDC in base piston.

4. CONCLUSIONS

A three-dimensional transient simulation with a knock model was performed to predict knock occurrence and autoignition site with three different piston shapes in a heavy-duty LPG engine. The major conclusions obtained are as follows:

(1) The decrease of turbulence intensity resulted from the smaller squish area made it possible to reduce knock occurrence in the heavy-duty LPG engine, which had a large combustion chamber. The modified piston was expected to restrain knock occurrence, while it had a rapid combustion characteristics like the bathtub piston.

(2) The combustion flame propagated toward the intake port side of the cylinder wall faster than other directions. In knock condition, autoignitions took place simultaneously in all the squish region. However, knock occurred mainly in the exhaust port side where the flame arrived later at the cylinder wall.

(3) This simulation method is a useful tool for engine development and makes it possible to predict the engine knock during the designing stage of the combustion chamber.

ACKNOWLEDGEMENT–The authors express their appreciation for the support of the Association of LPG Vehicles Supply Consultation (LG-Caltex Gas Co. and SK Gas Co.) and Korea Institute of Machinery & Materials.

REFERENCES

Adapco Software Limited. (1999). ProICE and ICE Version 4.0. Adapco Software Limited. New York.

AVL. (2000). BOOST User's Guide Version 3.3. AVL. Austria.

Choi, H., Hwang, S., Lee, J. and Min, K. (2002). 3-dimensional simulation of knock in a heavy-duty LPG engine. *SAE Technical Paper No.* 2002-01-2700.

Chun, K. M., Heywood, J. B. and Keck, J. C. (1988). Predictions of knock occurrence in a spark-ignition engine. *22nd Symposium on Combustion*, 455–463.

Chun, K. M. and Kim, K. W. (1994). Measurement and analysis of knock in an SI engine using the cylinder pressure and block vibration signals. *SAE Technical Paper No.* 940146.

Cowart, J. S., Keck, J. C. and Heywood, J. B. (1990). Engine knock predictions using a fully-detailed and a reduced chemical kinetics mechanism. *23rd Symposium on Combustion*, 1055–1062.

Dardalls, D., Matthews, R. D., Lewis, D. and Davis, K. (1998). The texas project, Part5-Economic analysis: CNG and LPG conversion of light-duty vehicle fleets. *SAE Technical Paper No.* 982447.

Heel, R., Maly, R., Weller, H. G. and Gosman, A. D., Validation of SI combustion model over range of speed, load, equivalence ratio and spark timing. *4th International Symposium COMODIA98*, 255–260.

Herweg, R. and Maly, R. (1992). A fundamental model for flame kernel formation in S. I. engines. *SAE Technical Paper No.* 922243.

Heywood, J. B. (1988). *Internal Combustion Engine Fundamentals.* Mc-Graw Hill. New York.

Hwan, S., Lee, J. and Min, K. (2001). The study on knock characteristics of heavy duty LPG engine. *Fall Conference Proc. Korean Society of Automotive Engineers*, 448–453.

Kamarados, P. (1994). Combustion modeling in internal combustion engines. *M. S. Dissertation, Imperial College.*

Kang, K. Y., Lee, D. Y., Oh, S. M. and Kim, C. U. (2001). Performance of a liquid phase LPG injection engine for heavy duty vehicles. *SAE Technical Paper No.* 2001-02-1958.

Kim, C. U., Lee, D. Y., Oh, S. M., Kang, K. Y., Choi, H. and Min, K. (2002). Enhancing performance and combustion of an LPG MPI engine for heavy duty vehicles. *SAE Technical Paper No.* 2002-01-0449.

Lee, J., Choi, H., Hwan, S. and Min. K. (2002). Study on the estimation of knock position in a LPG engine with ion-probe head gasket. *Spring Conference Proc. Korean Society of Automotive Engineers* 1486–1492.

Lee, Y., Pae, S., Min, K. and Kim, E. S. (2000). Prediction of knock onset and the autoignition site in spark-ignition engines. *Proc. Instn. Mech. Engrs.* **214D,** 751–763.

Pae, S. and Min, K. (2001). Modeling of laminar burning velocities for hydrocarbon and methanol fuels by using detailed chemical reaction mechanisms. *Trans. Korean Society of Mechanical Engineers,* **25,** 1303–1310.

Poinsot, T. J., Haworth, D. C. and Bruneaux, G. (1993). Direct simulation and modeling of flame-wall interaction for premixed turbulent combustion. *Combustion and Flame* **95,** 118–132.

Weller, H. G., Uslu, S., Gosman, A. D., and Maly, R. R. (1994). Predictions of combustion in homogeneous charge spark ignition engines. *3rd International Symposium COMODIA94*, 163–169.